Functional melanocytes derived from human pluripotent stem cells engraft into pluristratified epidermis

Xavier Nissan[a], Lionel Larribere[a], Manoubia Saidani[a], Ilse Hurbain[b,c,d], Cédric Delevoye[b,c], Jessica Feteira[e,f], Gilles Lemaitre[e,f], Marc Peschanski[e,f], and Christine Baldeschi[e,f,1]

[a]Centre d'Etude des Cellules Souches, I-Stem, Association Française Contre les Myopathies, 91030 Evry cedex, France; [b]Centre National de la Recherche Scientifique, Unité Mixte de Recherche 144 Institut Curie, Centre de Recherche, Paris F-75248, France; [c]Structure and Membrane Compartments and [d]Cell and Tissue Imaging Facility, [e]Institut National de la Santé et de la Recherche Médicale U-861, I-Stem, Association Française Contre les Myopathies, 91030 Evry cedex, France; and [f]University Evry Val d'Essonne U-861, I-Stem, Association Française Contre les Myopathies, 91030 Evry cedex, France

Edited by Rudolf Jaenisch, Whitehead Institute for Biomedical Research, Cambridge, MA, and approved July 22, 2011 (received for review December 20, 2010)

Melanocytes are essential for skin homeostasis and protection, and their defects in humans lead to a wide array of diseases that are potentially extremely severe. To date, the analysis of molecular mechanisms and the function of human melanocytes have been limited because of the difficulties in accessing large numbers of cells with the specific phenotypes. This issue can now be addressed via a differentiation protocol that allows melanocytes to be obtained from pluripotent stem cell lines, either induced or of embryonic origin, based on the use of moderate concentrations of a single cytokine, bone morphogenic protein 4. Human melanocytes derived from pluripotent stem cells exhibit all the characteristic features of their adult counterparts. This includes the enzymatic machinery required for the production and functional delivery of melanin to keratinocytes. Melanocytes also integrate appropriately into organotypic epidermis reconstructed in vitro. The availability of human cells committed to the melanocytic lineage in vitro will enable the investigation of those mechanisms that guide the developmental processes and will facilitate analysis of the molecular mechanisms responsible for genetic diseases. Access to an unlimited resource may also prove a vital tool for the treatment of hypopigmentation disorders when donors with matching haplotypes become available in clinically relevant banks of pluripotent stem cell lines.

ES cells | melanogenesis | cell therapy | BMP4

Molecular and cellular mechanisms of melanocyte development have been explored in a variety of species using experimental grafting and transgenesis, but the lack of appropriate technologies has greatly limited our knowledge of these mechanisms in humans to date. In vertebrates, melanocytes originate from migratory neural crest cells that emerge from the neural plate during embryogenesis (1, 2). Neural crest specification from the primitive ectoderm is regulated by bone morphogenic protein (BMP) and FGF signaling pathways (3, 4). Once committed, neural crest cells undergo a complex process of differentiation, proliferation, and migration out of the neural tube along defined pathways through the entire body to differentiate finally into numerous cell types, including melanocytes (5, 6). Multiple analyses of natural or induced mutation in mice have demonstrated that microphthalmia-associated transcription factor (*MITF*), paired box 3 (*PAX3*), sex-determining region Y-box 10 (*SOX10*), snail homolog 2 (*SNAIL2*), endothelin receptor (*EDNR*), and the tyrosine kinase receptor (*C-Kit*) play crucial roles in the control of neural crest cell migration, as well as in melanoblast specification, survival, and migration (7–11). How this relates to the human situation has only been accessible through correlations between mutant genes and disease phenotypes, as exemplified by the Waardenburg syndromes, which are associated with six genes of melanocytic differentiation: *PAX3*, *SOX10*, *MITF*, *EDNR*, endothelin-3 (*EDN3*), and *SNAIL2* (12, 13).

Pluripotent stem cells, either of embryonic origin or following genetic reprogramming, have already been widely used to model early stages of differentiation along a variety of lineages (14–16). In the case of melanocytes, a pioneering study was carried out using cocultures of mouse ES cells with the stromal cell line ST2 (17). This study confirmed that application of the known melanocyte activators stem cell factor (SCF), EDN3, 12-O-tetradecanoyl phorbol acetate (TPA), and dexamethasone (DEX) promotes cell differentiation. More recently, these studies have been extended to our species (18), showing a facilitating effect of WNT3a, EDN3, and SCF on the differentiation of human ES cells (hESCs). However, that study, which, to our knowledge, remains the only demonstration of hESC-derived melanocytes, was based on a first stage of differentiation requiring the formation of embryoid bodies and the secondary selection of pigmented cells. This has precluded any specific analysis of the hESC-to-melanocyte differentiation process itself, which is not accessible during the formation of the embryoid bodies.

We have reconsidered this issue here by taking the advantage of a finding made in a previous study that aimed at differentiating hESCs into another ectodermal derivative, namely, keratinocytes (19). Indeed, although keratinocytes formed 50–60% of the cells differentiated for 40 d from hESCs with high concentrations of BMP4 and ascorbic acid, the remaining cells comprised clusters of pigmented cells. Because most, if not all, of the cells in those cultures were ectodermal derivatives, it was hypothesized that they may be either neural crest-derived melanocytes or neuroectodermally derived retinal pigment epithelium cells (RPEs) (20). Analysis of morphological and molecular phenotypes has allowed us to separate two subpopulations of cells, with the specific characteristics of each phenotype. Melanocytes derived from pluripotent stem cells, both of embryonic origin and following genetic reprogramming of adult cells, were then further characterized phenotypically and functionally.

Results

Two different hESC lines (H9 and SA01) and one human induced pluripotent stem cell (iPSC) line were used in this study (cell line characterization is shown in Fig. S1). For the sake of clarity, the H9 cell line has been taken as a representative case in all following figures because results with the SA01 line were similar. Results obtained for the analyzed iPSC line, which were also altogether similar, are presented as supplementary data (*SI Methods*).

Author contributions: X.N., M.P., and C.B. designed research; X.N., L.L., M.S., I.H., C.D., and J.F. performed research; X.N., G.L., M.P., and C.B. analyzed data; and X.N., M.P., and C.B. wrote the paper.

The authors declare no conflict of interest.

This article is a PNAS Direct Submission.

[1]To whom correspondence should be addressed. E-mail: cbaldeschi@istem.fr.

This article contains supporting information online at www.pnas.org/lookup/suppl/doi:10.1073/pnas.1019070108/-/DCSupplemental.

BMP4-Mediated Control of Pluripotent Stem Cell Differentiation Along the Ectodermal Lineage. Undifferentiated pluripotent stem cells were seeded on mitomycin-treated 3T3 feeder cells in FAD medium and then supplemented with BMP4 and ascorbic acid for more than 40 d. The concentrations of BMP4 were gradually decreased to identify the optimal conditions for the derivation of neural crest progenitors (Fig. S2). The engagement of pluripotent stem cells at the earliest stage of cell commitment (10 d of differentiation) after treatment with different concentrations of BMP4 was evaluated using quantitative PCR. At that time point, hESCs were mostly engaged in epithelial commitment (*KRT18*$^+$, *p63*$^+$) at the highest concentrations of BMP4 tested (5–0.5 μM) (Fig. S2*A*). Neural crest cells (*HNK1*$^+$ and *p75*$^+$) were mostly generated when intermediate concentrations of BMP4 were used (0.02–0.004 μM). Neural cells (*SOX1*$^+$) were observed in large numbers at the lowest concentrations tested (0.004–0.0008 μM) (Fig. S2*B*). Results obtained with hESCs were similar for iPSCs. Morphological observations confirmed these results by showing the typical morphology of neural crest cells at an intermediate concentration of BMP4 in parallel with the loss of the typical epithelial morphology observed at a high concentration of BMP4 (Fig. S2*C*). Flow cytometry analysis confirmed the key role of an intermediate concentration of BMP4 for neural crest induction by revealing that a concentration of 0.02 μM increased the proportion of HNK1$^+$/p75$^+$ positive cells up to 36% (Fig. S2*D*). These data were confirmed by immunofluorescence using PAX3 antibodies (Fig. S2*E*). Moreover, inhibition of BMP signaling delayed differentiation of pigmented cells at the end of the process (Fig. S2*F*). Accordingly, BMP4 at a concentration of 0.02 μM was used in subsequent experiments on the neural crest-derived melanocytic lineage. Under these experimental procedures, pigmented cells appeared and progressively increased in number during the differentiation process. Morphological (Fig. 1*A*) and molecular (Fig. 1 *B–D*) characterization of pluripotent stem cell-derived pigmented cells was performed along the differentiation process. Quantitative PCR analysis showed a decrease in the pluripotency marker genes *OCT4*, *NANOG*, and *SOX2* (Fig. 1*B* and Fig. S3*A*) in parallel to an increase in the genes that encode the regulators of melanin synthesis: *TYRP1, TYROSINASE* (*TYR*), and *MITF* (Fig. 1*C* and Fig. S3*B*). The increase in the neural crest-derived cell markers *SOX10* and *PAX3* and the neural derivative marker *PAX6* was paralleled by enrichment of the cultures in the pigmented cells (Fig. 1*D*, Fig. S3*C*, and Table S1).

Derivation of a Pure Population of Melanocytes from Pluripotent Stem Cells. After 50 d of differentiation, the pigmented cells were mechanically isolated and subcultured in M254-CF medium (Invitrogen) suited to the survival of melanocytes (Fig. 1*E*). At this stage, the pigmented cells displayed two different morphologies. A first subpopulation exhibited epithelium-like structures, whereas a second one exhibited bipolar processes extending from a small ovoid cell body (Fig. 1*E*). In the first subpopulation, TYRP1 immunostaining coregistered with the typical markers of the RPEs, RPE 65 and PAX6, indicating its RPE-like phenotype (Fig. S4*A*). Accordingly, quantitative PCR showed an increase in both genes controlling melanin synthesis, *TYRP1* and *TYR*, and RPE markers, namely, *OTX2*, *BEST*, *RPE 65*, and the RPE-specific isoform of *MITF* (*MITF-D*) (Fig. S4*B*). In contrast, among the enriched pigmented cell population, 5–10% of the cells, depending on the cell line analyzed, expressed the neural crest lineage-specific marker PAX3, which was not expressed in hESC-derived RPEs (RPE-hESCs) (Fig. S4*C*). These cells corresponded to the non-pavimentous cell subpopulation, as shown after isolation by differential trypsinization and subculture in M254-CF medium. After 4 passages, cells exhibited a morphology similar to that of human epidermal melanocytes (HEMs) (Fig. 2*A* and Fig. S5*A*). Immunostaining analysis of these cells, subsequently called mel-hESCs and mel-iPSCs for "melanocytes derived from hESCs and iPSCs," revealed an appropriate cytoplasmic localization of TYRP1, TYR, S100, SILV, and Rab27 associated with a subcellular localization of PAX3, SLUG, and MITF in the nucleus and an absence of

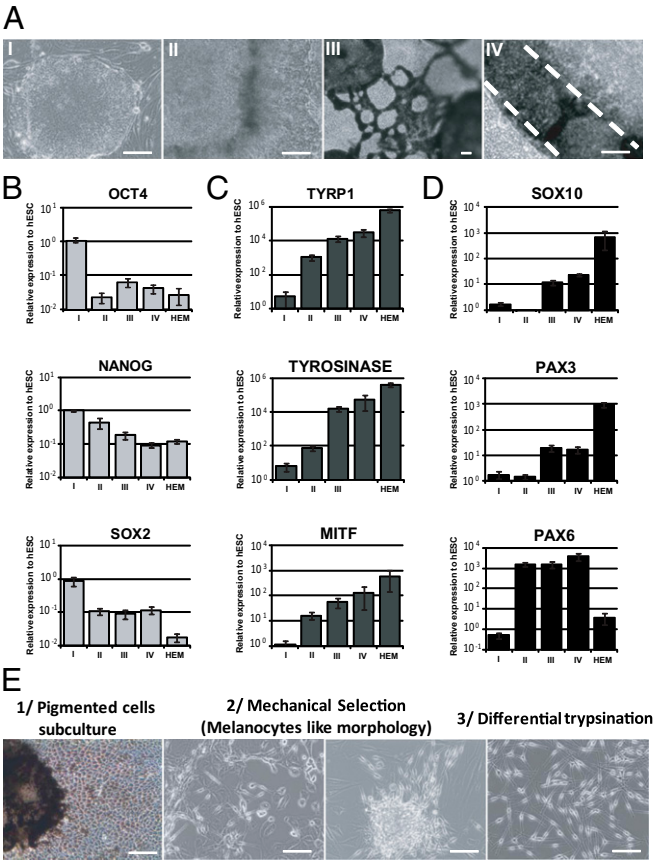

Fig. 1. Characterization of the hESC pigmentation process. (*A*) Microscopy analysis of undifferentiated hESCs (step I), hESC-derived cells before and after pigmentation (steps II and III, respectively), and enriched hESC-derived pigmented cells isolated at 60 d (step IV). (Scale bar: 50 μm.) (*B*) Quantitative PCR analysis of the pluripotency genes *OCT4, NANOG*, and *SOX2* during the hESC pigmentation process. (*C*) Quantitative PCR analysis of the melanogenesis-related genes *TYRP1, TYR*, and total *MITF* during the hESC pigmentation process. (*D*) Quantitative PCR analysis of the neural crest lineage *(SOX10* and *PAX3)* and neural lineage *(PAX6)* markers during the hESC pigmentation process. The data are normalized against 18S and expressed as relative expression to undifferentiated hESCs. HEMs were used as a control for adult melanocytes. Each bar represents the SEM (n = 3). (*E*) Schematic representation of the melanocytic enrichment procedure.

OCT4, TRA1-81, and PAX6 (Fig. 2*B* and Fig. S5*B*). These cells also demonstrated gene expression profiles similar to HEMs, as illustrated by the expression of *SOX10*, *PAX3*, the melanocyte-specific isoform of *MITF* (*MITF-M*), *TYRP1*, and *TYR*, associated with a background level of *PAX6*, *OTX2*, and *MITF-D* (Fig. 2*C* and Fig. S5*C*). FACS analysis after 4 passages confirmed the absence of SSEA4 and TRA1-81 expression (Fig. 2*D* and Fig. S5*D*). Conversely, more than 90% of these cells expressed TYRP1 and MITF (Fig. 2*D* and Fig. S5*D*). TaqMan array gene expression profiling, using a selected panel of 96 genes related to melanocyte biology, confirmed similar expression patterns of mel-hESCs, mel-iPSCs, and HEMs for a majority of genes (Fig. S5 *E* and *F* and Table S2). Mel-hESCs and mel-iPSCs could be propagated for up to 12 passages, frozen, and thawed without apparent changes in morphology (Fig. S6*A*), main phenotypic markers (Fig. S6*B*), cell proliferation rate (Fig. S6*C*), or mortality (Fig. S6*D*). Proliferation curves of HEMs, mel-hESCs, and mel-iPSCs were performed, revealing no differences in terms of proliferation rates between the source of melanocytes after 4 and 8 passages of cultures. Based on the flow cytometry cell quantification and subsequent calculation of their proliferation rate, we estimate the total number of melanocytes produced with this method at 2×10^4 to 10^5 at the first

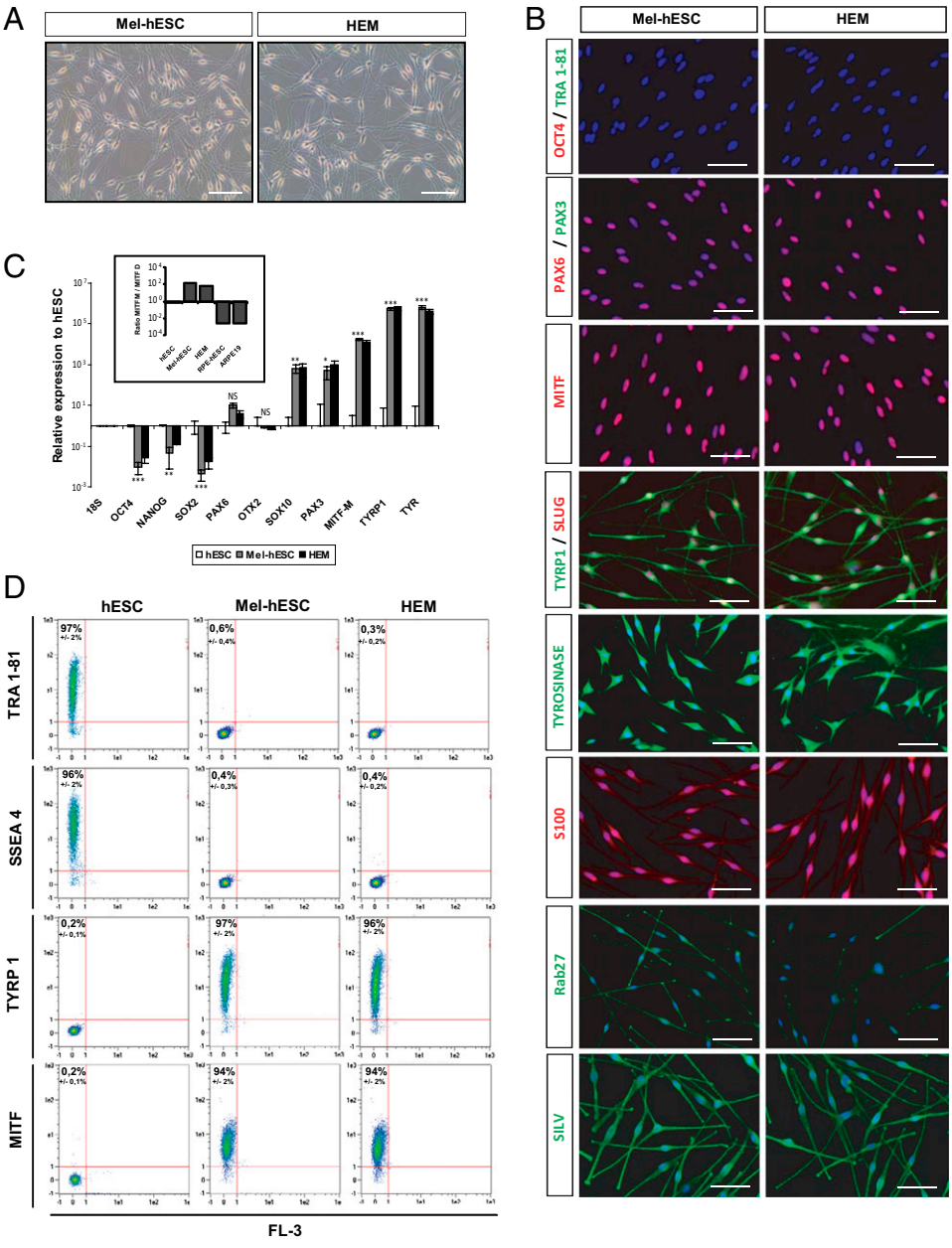

Fig. 2. Establishment of a homogeneous population of melanocytes derived from hESCs. (*A*) Microscopy analysis of HEM and mel-hESCs. (Scale bar: 50 μm.) (*B*) Immunofluorescence analysis of the pluripotency markers OCT4 and TRA1-81; the neural lineage marker PAX6; and the melanocyte markers PAX3, total MITF, TYRP1, SLUG, TYR S100, RAB2, and SILV in mel-hESCs and HEMs. (Scale bar: 50 μm.) (*C*) Quantitative PCR analysis of *OCT4*, *NANOG*, *SOX2*, *PAX6*, *OTX2*, *SOX10*, *PAX3*, *MITF-M* isoform, *TYRP1*, and *TYR* in mel-hESCs and HEMs. The data are normalized against 18S and expressed as relative expression to undifferentiated hESCs. Each bar represents the SEM (n = 3). $^{*}P < 0.05$; $^{**}P < 0.01$; $^{***}P < 0.001$; NS, not significant. Boxed histograms correspond to the ratio of *MITF-M* and MITF-*D* isoforms in hESCs, mel-hESCs, HEMs, RPE-hESCs, and ARPE-19 (adult RPE cell line). Each bar represents the SEM (n = 3). (*D*) FACS analysis of SSEA4, TRA1-81, TYRP1, and MITF in undifferentiated hESCs, mel-hESCs, and HEMs. Each value represents the SEM of three independent experiments. All data presented in this figure were obtained in melanocytes during four passages (approximately 50 d) after their isolation.

passage, which allows the total production of 10^8 melanocytes at passage 4 and at 2×10^{12} melanocytes at passage 8. Spinning-disk confocal microscopy and time-lapse recording revealed the presence of dark-containing organelles (Fig. 3*A*) that moved along the main axis of cell processes (Movies S1, S2, and S3). EM confirmed that the organelles present in mel-hESCs and mel-iPSCs were bona fide melanosomes at all stages of maturation, ranging from immature unpigmented (types I and II) up to mature melanin-containing (types III and IV) melanosomes (Fig. 3*B* and Fig. S7*A*).

Functional Characterization of Melanocytes Derived from Pluripotent Stem Cells. The functional status of melanocytes derived from pluripotent stem cells was first assessed by coculturing them with human adult keratinocytes. After 3 d of coculture, TYRP1/Keratin 14 (keratinocyte marker) coimmunostaining revealed $TYRP1^+$ organelles in keratinocytes when they had been cocultured with melanocytes and not in controls that were grown separately (Fig. 3*C* and Fig. S7*B*). $TYRP1^+$ organelles were localized in the perinuclear compartment of keratinocytes cocultured with mel-hESCs or mel-iPSCs, as well as in keratinocytes cocultured with HEMs. Automated quantification using the ArrayScan system (Cellomics) revealed about 20% $TYRP1^+$ keratinocytes in cocultures with either mel-hESCs or mel-iPSCs and up to 40% with HEMs (Fig. 3*D* and Fig. S7*C*). EM confirmed the presence of pigmented organelles in keratinocytes cocultured with either mel-hESCs or mel-iPSCs (Fig. 3 *E* and *F* and Fig. S7 *D* and *E*). Further functional evaluation of mel-hESCs was sought using the 3D reconstruction of a pluristratified epidermis in vitro, by mixing melanocytes with adult basal keratinocytes seeded as a monolayer on a matrix at the medium-air interface (Fig. 4). After the development of a fully pluristratified epidermis, macroscopic observation revealed pigmentation in the reconstructed tissue that contained melanocytes. Fontana–Masson staining and TYRP1 immunostaining confirmed the presence of melanin-containing cells in the basal layer of the epidermis (Fig. 4*A*). In upper layers of the reconstructed epidermis, melanin-containing processes intermingled with keratinocytes. Treatment of the melanized epidermis with α-melanocyte stimulating hormone enhanced the production of melanin in the reconstructed tissue (Fig. 4*B*).

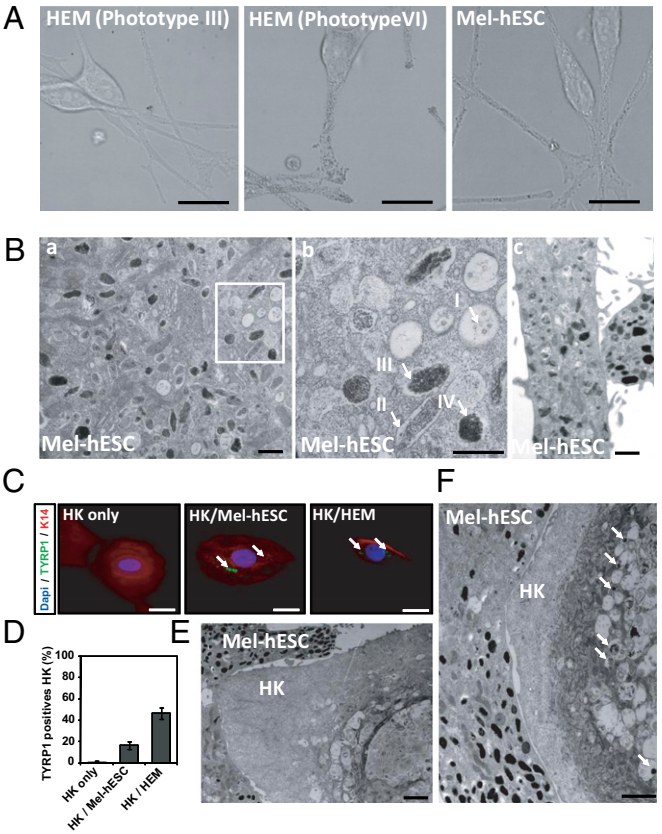

Fig. 3. Biogenesis and maturation of melanosomes in melanocytes derived from hESCs. (*A*) Spinning-disk confocal microscopy was used to capture high-resolution pigmented melanosomes in HEMs (phototypes III and VI) and mel-hESCs. (Scale bar: 5 μm.) (*B*) EM of mel-hESCs. Characteristic immature and mature melanosomes are observed in the cell soma (*a*) and processes in the dendrites (*c*). (*b*) Higher magnification of the boxed area in *a*. Arrows represent the different types of melanosomes. (Scale bar: 400 nm.) (*C*) Immunofluorescence analysis of keratin 14 (K14) and TYRP1 in keratinocytes after 3 d of coculture: without melanocytes (*Left*), with mel-hESCs (*Center*), and with HEMs (*Right*). HK, human keratinocyte. (Scale bar: 10 μm.) (*D*) ArrayScan automated quantification of the percentage of TYRP1$^+$ keratinocytes after 3 d of coculture with melanocytes (left to right): without melanocytes, with mel-hESCs, and with HEMs. Each bar represents the SEM for three experiments. For each experiment, 100 cells were analyzed. (*E* and *F*) EM of a keratinocyte after 3 d of coculture with mel-hESCs. Arrows represent transferred pigment into keratinocytes. (Scale bar: 400 nm.) All data presented in this figure were obtained in melanocytes during four passages (approximately 50 d) after their isolation.

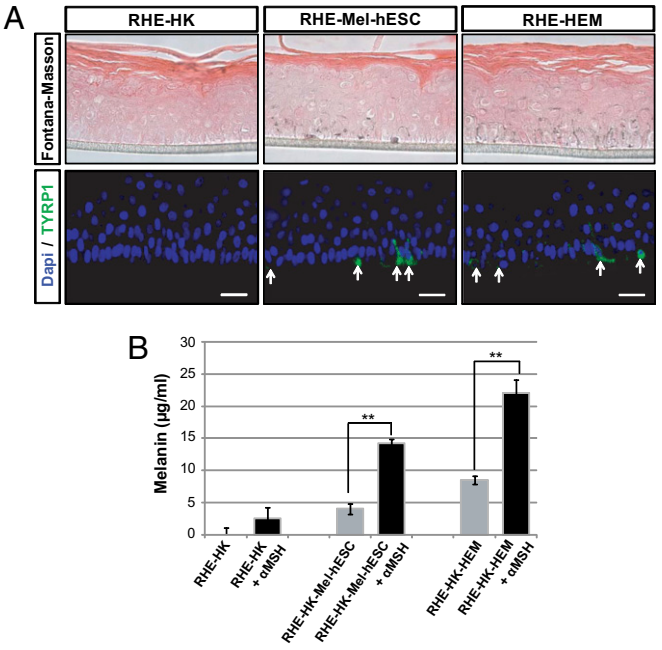

Fig. 4. Morphological and functional characterization of melanocytes derived from hESCs in an in vitro model of reconstituted melanized epidermis. (*A*) Fontana–Masson and TYRP1 immunofluorescence staining on reconstituted human epidermis without melanocytes (RHE-HK), containing mel-hESCs (RHE-mel-hESC) or HEMs (RHE-HEM). (Scale bar: 50 μm.) (*B*) Quantification of melanin content (μg/mL) from reconstituted epidermis containing or not containing melanocytes, without or with stimulation by 1 μM α-melanocyte stimulating hormone (left to right): without melanocytes, with mel-hESCs, and with HEMs. α-MSH, α-melanocyte stimulating hormone. Bars represent the SEM for three experiments (**$P < 0.01$). All data presented in this figure were obtained in melanocytes during four passages (approximately 50 d) after their isolation.

Discussion

The main result of this study is the in vitro generation of functional melanocytes from pluripotent stem cells, both hESCs and iPSCs, capable of producing melanin that can be taken up by keratinocytes in cocultures. The availability of human cells committed to the melanocytic lineage in vitro, at all stages of differentiation, will enable investigation of those mechanisms that guide the developmental processes and may provide evidence of the human equivalent of melanoblasts, which has remained elusive up to now. In parallel, our results will facilitate the in vitro analysis of those molecular mechanisms that underlie the melanocytic defects observed in genetic diseases. Lastly, the demonstrated functional integration of melanocytes derived from hESC and iPSC lines into reconstituted pluristratified epidermis potentially paves the way for promoting cell therapy in hypopigmentation disorders, such as vitiligo. Human melanocytes were derived here in vitro from undifferentiated pluripotent stem cells using a moderate concentration of BMP4. This protocol, in contrast to previous ones that relied on embryoid bodies, enables the engagement of the cells into the neural crest lineage to be followed step by step and, subsequently, the specification of the terminally differentiated cells. This offers a convenient model for the study of the molecular mechanisms underlying melanocyte development. Many reports support the idea that a gradient of BMP activity is the crucial point for division of the ectoderm into the neural plate, neural crest, and epidermis (21). It has been shown in *Xenopus* and zebrafish models that a gradient of BMP is able to specify the neural plate border, including neural crest cells (21). More precisely, Tribulo et al. (22) demonstrated that a specific level of BMP4 activity leads to the *SLUG* expression implicated in melanocytic development. Lower or higher amounts of BMP4 failed to induce *SLUG* expression, confirming previous reports of induction of the neural crest by a gradient of BMP (22). Molecularly, BMP4 signaling activates *SLUG* promoter activity in the neural crest through direct binding of the phosphorylated BMP signal transducer Smad1 (23). This Smad activation induces apoptotic cell death of neuroectodermal precursor cells already engaged in the neural cell fate. BMP4 assayed on mouse ES cell differentiation induced a dramatic apoptotic death of Sox-1$^+$ neural precursors with a concomitant epidermal engagement (24). In 2007, a pioneer study demonstrated that activation of BMP signaling could permit the differentiation of human pluripotent stem cells into neural crest stem cells through the generation of neural rosettes (25). BMP provoked a significant increase in HNK1$^+$/p75$^+$ neural crest precursors, which could be reversed using a BMP antagonist (25). Altogether, these findings indicate that neural crest precursors can emerge from

hESC-derived neural rosettes through a BMP treatment. In our study, we optimized the concentration of BMP4 to potentialize the neural crest commitment of human pluripotent stem cells. The molecular mechanisms by which different levels of BMP activate a diversity of pathways of differentiation are yet to be defined, and our in vitro model may offer a path for such a study. Molecular mechanisms and genetic pathways involved in melanocyte development were originally described in chicken models using chimeras (26, 27). These pioneer studies demonstrated that melanocytes initially derive from a group of migratory embryonic cells referred to as the neural crest, which secondarily mature under the control of BMPs, Wnt/β-catenin, and FGFs into pigmented progenitors (28). Several studies, mainly performed on the mouse, have shown that melanocytic development depends on two key signaling systems, namely, the Kit and the G protein-coupled endothelin receptor B (EDNRB) pathways (27). Because of the absence of an in vitro model of human melanocyte development, it has not been possible to ascribe many factors to the specification of the melanocytic lineage in our species. Thus, the development of a new model of melanocyte differentiation that reproduces the chronobiology of human development appears to be crucial to the exploration of those yet unknown molecular mechanisms that control melanocyte differentiation. In vitro modeling of melanocyte development has been performed by Kunisada and colleagues (17) on mouse ES cells. It relied on a protocol using cocultures with ST2 stromal cells and a complex array of factors and cytokines that included SCF, EDN3, and endogenous ligands of c-Kit and EDNRB receptors, associated with DEX, basic FGF, cholera toxin (CT), and TPA. By adapting this protocol to the humans, Fang et al. (18) and Zabierowski and Herlyn (29) were able to obtain melanocytes from hESCs, forcing melanocytic differentiation with SCF, END3, and Wnt3a. However, this protocol involved the obligatory formation of embryoid bodies as a first stage in the differentiation of undifferentiated hESCs, and thus precluded discrete analysis of the molecular mechanisms leading to lineage commitment. Moreover, in addition to its altogether complex cytokinic treatment, the authors (18, 29) highlighted the fact that this protocol required a nonphysiological concentration of Wnt3a to engage this differentiation process. In contrast, here, what we have described is a directed protocol that enables the generation of melanocytes from hESCs and iPSCs without either the formation of embryoid bodies or heavy cytokinic treatments to commit the undifferentiated cell to the neural crest lineage, based on a moderate concentration of BMP4 (30). This opens up the possibility of a discrete analysis of the first steps of commitment leading to melanocytes in the humans, including the characterization of the intermediate stage of melanoblasts that has been characterized in the mouse (31). If this stage does exist in our species, it has not yet been described. Dysfunction and loss of melanocytes lead to several defects known as UV-induced hypersensitivity pigmentary disorders, some of which have very high morbidity or may transform into melanoma, which is one of the most severe types of cancer. Molecular mechanisms at the source of these disorders are frequently not well characterized. Over the past 20 y, progress has been made in understanding these diseases, largely as a result of parallel studies of human patients and inbred mice with similar phenotypes, allowing, in particular, an indication of the functional alteration of melanocytes in the cases of albinism, Griscelli syndrome, or Hermansky–Pudlak syndrome, which exhibit defects in melanin production and transfer (32, 33). Direct analysis of pathological mechanisms in human cells has, in contrast, remained hampered by difficulties in accessing a relevant biological resource. The derivation of melanocytes from human pluripotent stem cells meets that need insofar as these cell lines can be obtained from donors with specified genotypes of interest and, as such, may provide cellular models of genetic diseases. Human pluripotent stem cell lines have been considered as potentially providing unique models for human diseases since the initial derivation of an hESC line (34). Preimplantation genetic diagnosis (PGD) opened up the possibility of prospectively identifying embryos with particular genetic disorders and then deriving "disease-specific" hESCs [e.g., for Huntington disease (35), fragile X syndrome (36), myotonic dystrophy type 1 (37)]. More recently, human iPSCs have broadened the pathological modeling of pluripotent stem cells to virtually all other monogenic diseases for which PGD was not available (38, 39). There have already been attempts to establish disease models through patient-specific reprogramming in a search for molecular mechanisms associated with diseases [e.g., Parkinson disease (40), spinal muscular atrophy (41), amyotrophic lateral sclerosis (42)]. Our results open the way to extending those studies to pigmentary disorders by providing an accurate protocol for differentiating iPSCs from patients as well as hESCs from PGD embryos into functional melanocytes. The analysis of defective molecular mechanisms is able to target cell-autonomous defects in the specific machinery associated with melanocyte differentiation and function. Indeed, the melanocytes derived here from human pluripotent stem cells expressed all the tested genes that regulate key processes involved in pigmentation as well as in neural crest development, melanin synthesis, and melanosome transfer. As in all other types of differentiation from pluripotent stem cell lines, however, it remains to be established how the "theoretical age" of the cells, taking the undifferentiated stage as equivalent to a first-week blastocyst, influences their phenotype, compared with cells directly obtained from adult donors. The observation that the melanin content transfer, although present, may be quantitatively less efficient for hESC- and iPSC-derived melanocytes may relate to such a difference in overall maturation. In addition to cell-autonomous mechanisms, the results obtained in the present study open the way to analyses of cell-to-cell interaction in an organotypic epidermal context. Reconstructing epidermis in vitro with melanocytes and keratinocytes derived from individuals with unique genotypes of interest may also be of major importance in the analysis of those mechanisms underlying differential sensitivity to UV stress or chemical toxicity (43). Cell therapy utilizing melanocytes has been used experimentally for years as an adjunct treatment for the hypopigmentary disorder vitiligo (44). Vitiligo affects 1% of the world's population and is associated with high morbidity, particularly psychiatric complications. It is an autoimmune disease characterized by a progressive loss of skin pigmentation caused by the infiltration of $CD4^+$ and $CD8^+$ T lymphocytes into the skin and loss of melanocytes (45). This forces patients to apply UV protection continuously to the affected areas. Over the past 10 y, many treatments have been tried, such as topical steroids, psoralen and UV A light, narrow band UV B light, vitamin D analogs, or pseudocatalase (44). These treatments have demonstrated partial efficiency but were marred by adverse effects. This has led to cell therapy attempts based on either skin autografts or infiltration of autologous melanocytes, whether grown in culture or not and, on occasion, associated with keratinocytes (46). To date, these surgical attempts have been applied only to small skin areas because of limited access to cells and tissues. Melanocytes derived from pluripotent stem cells would clearly address this issue of accessibility and help extend those surgical treatments to a much larger group of patients.

Methods

Pluripotent Stem Cell Culture and Melanocyte Differentiation. hESCs from two cell lines, SA01 (Cellartis) and H9 (Wicell), were grown on STO (ATCC) mouse fibroblasts, inactivated with 10 mg/mL mitomycin C, seeded at 30,000 per cm^2, and grown as previously described (19). In addition, one human iPSC line was derived from adult skin fibroblasts (Coriell Institute) using Yamanaka's original method with *OCT4*, *KLF4*, *SOX2*, or *CMYC* transferred using retroviral vectors (16). The iPSC line was amplified up to the 15th passage before differentiation. For differentiation, hESC and iPSC clumps were seeded onto mitomycin C-treated 3T3 fibroblasts in FAD medium composed of 2/3 DMEM, 1/3 HAM/F12 Nutrient mixture, and 10% (vol/vol) FCS (FCII; HyClone) supplemented with 5 μg/mL insulin, 0.5 μg/mL hydrocortisone, 10^{-10} M CT, 1.37 ng/mL triiodothyronine, 24 μg/mL adenine, and 10 ng/mL recombinant human EGF. Three independent experiments were performed using each pluripotent cell line. Induction of ectodermal differentiation was obtained by a treatment using 20 nM human recombinant BMP4 (R&D) and 0.3 mM

DEVELOPMENTAL BIOLOGY

ascorbic acid (Sigma–Aldrich). Cells were grown in the same medium until clones of pigmented populations were observed and isolated. After selection, pigmented cells were dissociated using 0.05% trypsin (Invitrogen) and seeded as single cells in M254-CF medium (Invitrogen) supplemented with human melanocyte growth factor supplements (Invitrogen) suitable for melanocyte culture. After 2 wk of culture in these conditions, cells presenting a morphology similar to that of melanocytes were mechanically isolated based on their morphology and amplified separately in the same medium for up to 12 passages using rapid differential trypsinization. All the molecular characterization of mel-hESCs and mel-iPSCs was systematically performed during 4 passages after isolation.

ACKNOWLEDGMENTS. The authors thank Cécile Denis, Christine Varela, Yves Maury, Dr. Graca Raposo, Dr. Mathilde Girard, Dr. Yacine Laabi, and the StratiCELL company for their part in certain experiments and Dr. Cécile Martinat for revising the manuscript and providing helpful discussions. This work was supported by the Institut National de la Santé et de la Recherche Médicale, University Evry Val d'Essonne, Association Française Contre les Myopathies, and Genopole.

1. Bronner-Fraser ME, Cohen AM (1980) The neural crest: What can it tell us about cell migration and determination? *Curr Top Dev Biol* 15:1–25.
2. Bronner ME, Cohen AM (1979) Migratory patterns of cloned neural crest melanocytes injected into host chicken embryos. *Proc Natl Acad Sci USA* 76:1843–1847.
3. Marchant L, Linker C, Ruiz P, Guerrero N, Mayor R (1998) The inductive properties of mesoderm suggest that the neural crest cells are specified by a BMP gradient. *Dev Biol* 198:319–329.
4. Villanueva S, Glavic A, Ruiz P, Mayor R (2002) Posteriorization by FGF, Wnt, and retinoic acid is required for neural crest induction. *Dev Biol* 241:289–301.
5. Le Douarin NM (2004) The avian embryo as a model to study the development of the neural crest: A long and still ongoing story. *Mech Dev* 121:1089–1102.
6. Erickson CA, Reedy MV (1998) Neural crest development: The interplay between morphogenesis and cell differentiation. *Curr Top Dev Biol* 40:177–209.
7. Wehrle-Haller B (2003) The role of Kit-ligand in melanocyte development and epidermal homeostasis. *Pigment Cell Res* 16:287–296.
8. Wehrle-Haller B, Weston JA (1995) Soluble and cell-bound forms of steel factor activity play distinct roles in melanocyte precursor dispersal and survival on the lateral neural crest migration pathway. *Development* 121:731–742.
9. Lee HO, Levorse JM, Shin MK (2003) The endothelin receptor-B is required for the migration of neural crest-derived melanocyte and enteric neuron precursors. *Dev Biol* 259:162–175.
10. Hornyak TJ, Hayes DJ, Chiu LY, Ziff EB (2001) Transcription factors in melanocyte development: Distinct roles for Pax-3 and Mitf. *Mech Dev* 101:47–59.
11. Cheli Y, Ohanna M, Ballotti R, Bertolotto C (2010) Fifteen-year quest for microphthalmia-associated transcription factor target genes. *Pigment Cell Melanoma Res* 23:27–40.
12. Waardenburg PJ (1951) A new syndrome combining developmental anomalies of the eyelids, eyebrows and nose root with pigmentary defects of the iris and head hair and with congenital deafness. *Am J Hum Genet* 3:195–253.
13. Asher JH, Jr., Friedman TB (1990) Mouse and hamster mutants as models for Waardenburg syndromes in humans. *J Med Genet* 27:618–626.
14. Maherali N, Hochedlinger K (2008) Guidelines and techniques for the generation of induced pluripotent stem cells. *Cell Stem Cell* 3:595–605.
15. Thomson JA, et al. (1998) Embryonic stem cell lines derived from human blastocysts. *Science* 282:1145–1147.
16. Takahashi K, et al. (2007) Induction of pluripotent stem cells from adult human fibroblasts by defined factors. *Cell* 131:861–872.
17. Yamane T, Hayashi S, Mizoguchi M, Yamazaki H, Kunisada T (1999) Derivation of melanocytes from embryonic stem cells in culture. *Dev Dyn* 216:450–458.
18. Fang D, et al. (2006) Defining the conditions for the generation of melanocytes from human embryonic stem cells. *Stem Cells* 24:1668–1677.
19. Guenou H, et al. (2009) Human embryonic stem-cell derivatives for full reconstruction of the pluristratified epidermis: A preclinical study. *Lancet* 374:1745–1753.
20. Idelson M, et al. (2009) Directed differentiation of human embryonic stem cells into functional retinal pigment epithelium cells. *Cell Stem Cell* 5:396–408.
21. LaBonne C, Bronner-Fraser M (1998) Neural crest induction in Xenopus: Evidence for a two-signal model. *Development* 125:2403–2414.
22. Tribulo C, Aybar MJ, Nguyen VH, Mullins MC, Mayor R (2003) Regulation of Msx genes by a Bmp gradient is essential for neural crest specification. *Development* 130: 6441–6452.
23. Sakai D, et al. (2005) Regulation of Slug transcription in embryonic ectoderm by beta-catenin-Lef/Tcf and BMP-Smad signaling. *Dev Growth Differ* 47:471–482.
24. Gambaro K, Aberdam E, Virolle T, Aberdam D, Rouleau M (2006) BMP-4 induces a Smad-dependent apoptotic cell death of mouse embryonic stem cell-derived neural precursors. *Cell Death Differ* 13:1075–1087.
25. Lee G, et al. (2007) Isolation and directed differentiation of neural crest stem cells derived from human embryonic stem cells. *Nat Biotechnol* 25:1468–1475.
26. Le Douarin NM (1980) The ontogeny of the neural crest in avian embryo chimaeras. *Nature* 286:663–669.
27. Tachibana M, Kobayashi Y, Matsushima Y (2003) Mouse models for four types of Waardenburg syndrome. *Pigment Cell Res* 16:448–454.
28. Kanzler B, Foreman RK, Labosky PA, Mallo M (2000) BMP signaling is essential for development of skeletogenic and neurogenic cranial neural crest. *Development* 127: 1095–1104.
29. Zabierowski SE, Herlyn M (2010) Embryonic stem cells as a model for studying melanocyte development. *Methods Mol Biol* 584:301–316.
30. Fuchs S, Sommer L (2007) The neural crest: Understanding stem cell function in development and disease. *Neurodegener Dis* 4:6–12.
31. Thomas AJ, Erickson CA (2008) The making of a melanocyte: The specification of melanoblasts from the neural crest. *Pigment Cell Melanoma Res* 21:598–610.
32. Griscelli C, et al. (1978) A syndrome associating partial albinism and immunodeficiency. *Am J Med* 65:691–702.
33. Beermann F, et al. (1990) Rescue of the albino phenotype by introduction of a functional tyrosinase gene into mice. *EMBO J* 9:2819–2826.
34. Gearhart J (1998) New potential for human embryonic stem cells. *Science* 282: 1061–1062.
35. Mateizel I, et al. (2006) Derivation of human embryonic stem cell lines from embryos obtained after IVF and after PGD for monogenic disorders. *Hum Reprod* 21:503–511.
36. Eiges R, et al. (2007) Developmental study of fragile X syndrome using human embryonic stem cells derived from preimplantation genetically diagnosed embryos. *Cell Stem Cell* 1:568–577.
37. Marteyn A, et al. (2011) Mutant human embryonic stem cells reveal neurite and synapse formation defects in type 1 myotonic dystrophy. *Cell Stem Cell* 8:434–444.
38. Wernig M, Meissner A, Cassady JP, Jaenisch R (2008) c-Myc is dispensable for direct reprogramming of mouse fibroblasts. *Cell Stem Cell* 2:10–12.
39. Saha K, Jaenisch R (2009) Technical challenges in using human induced pluripotent stem cells to model disease. *Cell Stem Cell* 5:584–595.
40. Wernig M, et al. (2008) Neurons derived from reprogrammed fibroblasts functionally integrate into the fetal brain and improve symptoms of rats with Parkinson's disease. *Proc Natl Acad Sci USA* 105:5856–5861.
41. Ebert AD, et al. (2009) Induced pluripotent stem cells from a spinal muscular atrophy patient. *Nature* 457:277–280.
42. Dimos JT, et al. (2008) Induced pluripotent stem cells generated from patients with ALS can be differentiated into motor neurons. *Science* 321:1218–1221.
43. Cario-André M, et al. (1999) The reconstructed epidermis with melanocytes: A new tool to study pigmentation and photoprotection. *Cell Mol Biol (Noisy-le-grand)* 45: 931–942.
44. Abu Tahir M, Pramod K, Ansari SH, Ali J (2010) Current remedies for vitiligo. *Autoimmun Rev* 9:516–520.
45. Badri AM, et al. (1993) An immunohistological study of cutaneous lymphocytes in vitiligo. *J Pathol* 170:149–155.
46. Khunger N, Kathuria SD, Ramesh V (2009) Tissue grafts in vitiligo surgery—Past, present, and future. *Indian J Dermatol* 54:150–158.